Lifetime Evaluation of Orthotropic Steel Bridge Decks

Koichi Sugioka*, Gregory A. MacRae**, Mofreh Saleh***, Mike Beamish****

*Ph.D. Candidate, Department of Civil and Natural Resources Engineering, University of Canterbury, Private Bag 4800 Christchurch 8020, New Zealand; PH. +64 3 3642987 ext. 7312; ksu40@student.canterbury.ac.nz
**Associate Professor, Department of Civil and Natural Resources Engineering, University of Canterbury, Private Bag 4800 Christchurch 8020, New Zealand; PH. +64 3 3642247; gregory.macrae@canterbury.ac.nz
***Senior Lecturer, Department of Civil and Natural Resources Engineering, University of Canterbury, Private Bag 4800 Christchurch 8020, New Zealand; PH. +64 3 3642987 ext. 7339; mofreh.saleh@canterbury.ac.nz
****Associate - Civil Structures, Beca Infrastructure Ltd; PH. +64 9 300 9000; mike.beamish@beca.com

Abstract

The fatigue performance of orthotropic steel bridge decks depends on the magnitude and number of stress cycles applied, and the deck details. The stress induced in a deck plate will be reduced by the presence of a stiff surfacing material. This paper describes how the likely fatigue lifetime of an orthotropic steel bridge deck with asphalt surfacings could be estimated using probabilistic assessment methodology. In particular, the daily variations in temperature, which affect the asphalt surfacings, are considered. An example of application of the methodology to a realistic bridge is described.

Introduction

Orthotropic steel bridge decks have been selected in the design of long span steel bridges because of their favourable characteristics of their high longitudinal stiffness, light weight and short installation time. Two basic types of longitudinal ribs are used; open ribs, and closed ribs of a trapezoidal or rounded cross section. The closed ribs are more commonly used than the open ribs because open ribs are less torsionally rigid and require more welding. Fatigue cracks, however, have often developed at welded connections in orthotropic steel bridges with closed ribs due to the high number of high magnitude axle loads. Many relevant investigations have been conducted internationally (e.g. Wolchuk 1990; Beamish et al. 2006; Jong 2006; Miki 2006; Sugioka et al. 2007). Six locations of fatigue cracks have been identified (Kolstein 2007): (1) at the welded joint between the deck plate and the longitudinal rib between the crossbeams; (2) at the welded joint between the deck plate and the longitudinal rib at the crossbeam; (3) at the longitudinal rib splice welded joint; (4) at the welded joint between the longitudinal rib and the crossbeam; (5) at the welded joint between vertical stiffener and deck plate; and (6) at the butt welded joint in the

deck plate. The rib-to-deck joints (crack type 1 and 2) have four types of potential fatigue cracks as shown in Figure 1: (A) propagating from the weld root through the deck plate; (B) propagating from the weld root through the weld throat; (C) propagating from the weld toe in the deck plate through the deck plate; (D) propagating from the weld toe in the longitudinal rib through the longitudinal rib. The rib-to-deck joints are generally prone to fatigue failures due to out-of-plane bending moments in the deck plates and longitudinal ribs generated by axle loads. Out-of-plane bending moments result in high local flexural stresses in the deck plates and longitudinal ribs since thicknesses of the deck plates and rib walls are relatively thin.

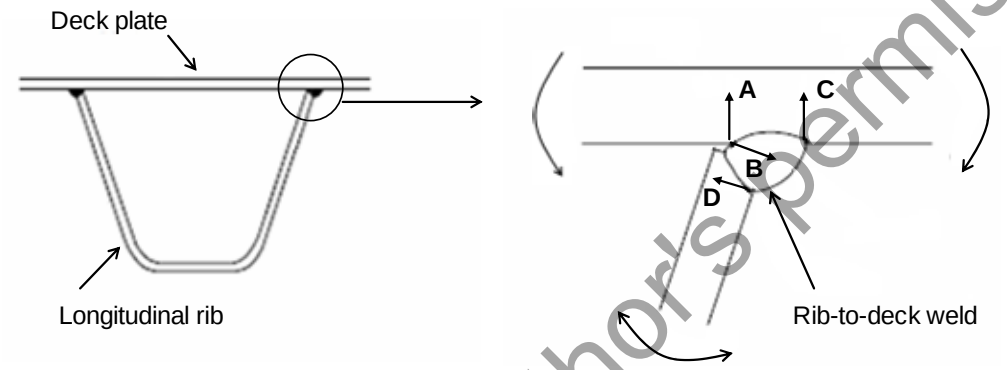

Figure 1 Fatigue cracks at rib-to-deck joint.

Fatigue is important for many steel bridge structures, but there are numerous uncertainties in definitions when failure occurs. Current conventional design of steel bridges and fatigue analysis is usually based on *S-N* curves and the Palmgren–Miner hypothesis. In reality, however, the *S-N* curves are only available for a limited number of structural details, stated by classification tables of design codes. The conditions governing fatigue cracking are generally the structural geometry, material characteristics, and loadings. These conditions are difficult to assess accurately. Thus, an appropriate analysis of fatigue is required to treat the problem in a probabilistic manner. Temperature effects on asphalt surfacing are also not generally considered in conventional design.

The proposed approach to assess fatigue lifetime to cracking has similarities to the Pacific Earthquake Engineering Research (PEER) performance-based earthquake engineering (PBEE) methodology. An example application of the methodology to the rib-to-deck welded joints of a realistic bridge using Monte Carlo simulation with one thousand samples is described to predict the remaining lifetime considering hourly temperature effects under each condition.

Probabilistic Fatigue Assessment Methodology for Orthotropic Bridge Decks

An approach using the basic concept that needed for fatigue assessment has already been developed with respect to earthquakes (Cornell and Krawinkler 2000). The PEER framing equation can be given by

$$\lambda(DV) = \int_{DM}\int_{EDP}\int_{IM} G(DV \mid DM)\left|dG(DM \mid EDP)\right|\left|dG(EDP \mid IM)\right|\left|d\lambda(IM)\right| \quad (1)$$

where DV = decision variable; DM = damage measure; EDP = engineering demand parameter; IM = intensity measure; $G(x|y) = P(x<X|Y=y)$ = the conditional complementary cumulative distribution function of X given Y; $\lambda(x)$ = the mean annual frequency of exceeding x. Terminology on seismic loss assessment can be compared as shown in Table 1; the intensity measure and the engineering demand parameter may be equivalent to an axle weight and a stress range respectively. The damage measure may be equivalent to damage in the Palmgren–Miner hypothesis. Repeated simulations can yield a distribution of the fatigue lifetime to failure on a particular point on the bridge.

Table 1 Comparison of measures between the PEER approach and fatigue assessment.

	Intensity Measure	Engineering Demand Parameter	Damage Measure	Decision Variable
	IM	EDP	DM	DV
Seismic	Spectral acceleration	e.g. Story drift	e.g. Number of cracks/fracture	$
Fatigue	Traffic loading (e.g. Axle weight)	Nominal stress	Formed from S-N curves	$

Details Required for Bridge Lifetime Evaluation

Fatigue lifetime can be defined as the length of time before fatigue cracking at a welded joint in this paper. The fatigue lifetime is expressed in terms of remaining years.

As an example, the proposed probabilistic fatigue assessment methodology is applied to the rib-to-deck welded joints of the Shinhamadera Bridge which had a fatigue crack (crack type A in Figure 1) in a longitudinal rib-to-deck welded joint (Sugioka et al. 2007). A schematic illustration of the eight-step process in the fatigue assessment is given in Figure 2. Framed values in this figure are obtained using a Monte Carlo Simulation method. The lifetime assessment includes:

Step 1: Select steel member properties;
Step 2: Calculate yearly temperatures, and traffic growth;
Step 3: Calculate hourly temperatures, asphalt elastic moduli and stress reduction;
Step 4: Calculate axle weights, and transverse positions of axle loads;
Step 5: Calculate stress ranges from the axle weight data;
Step 6: Calculate damage from the stress range data;
Step 7: Calculate fatigue lifetime from the damage data;
Step 8: Repeat from step 1 to step 7 for a fatigue lifetime distribution.

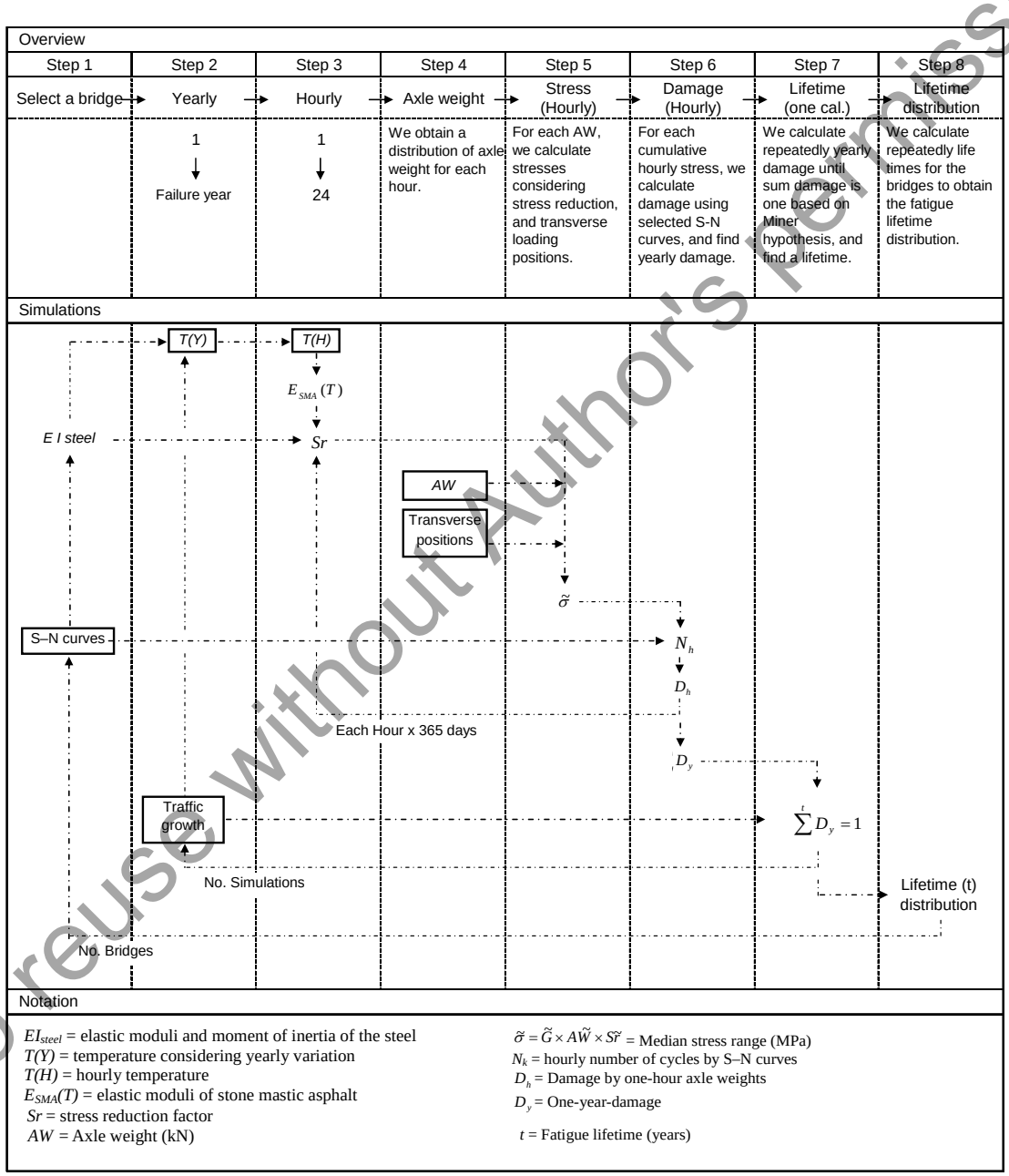

Figure 2 Schematic illustration of the probabilistic fatigue assessment methodology for orthotropic steel bridge decks.

Step 1: Select steel member properties. For each simulation, a bridge is firstly selected. Elastic moduli and moment of inertia of steel members are determined by properties of the selected steel bridge members. The elastic modulus for steel is assumed to be 210,000 MPa in this study.

An *S-N* line is also obtained from the selected steel bridge members as it assumed that the steel bridge is fabricated using the same materials and welding. The design *S-N* line is defined as the mean *S-N* line minus two times the standard deviation, which is represented by

$$\log \tilde{N} = \log A - B \log S + 2\beta \tag{2}$$

where $\tilde{N}$ = number of cycles to failure of a stress ranges, S; A = constant term relating to the mean-line minus two standard deviations used in design codes (3.91×10^{12} for Detail Category 125, 2.00×10^{12} for Detail Category 100, 7.16×10^{11} for Detail Category 71 in e.g. EN1993-1-9 (2005)); B = inverse slope of the *S-N* curve (3 in e.g. EN1993-1-9 (2005)); β = standard deviation of log N. In this assessment, the rib-to-deck welded joints in an orthotropic steel deck would be separately regarded as Detail Categories 125, 100, or 71 to comply with Eurocode 3 (EN1993-1-9 2005) with a standard deviation of 0.207, which is the average standard deviation between Classes C and W according to BS5400 (1980). Detail Category 125 has been recommended by Kolstein (2007), Detail Category 100 has been described for the critical regions at the longitudinal rib-to-deck welded joint in prEN1993-2 (2005), and Detail Category 71 has been specified in EN1993-1-9 (2005).

Step 2: Calculate yearly temperatures and traffic growth. Figure 3 shows the yearly temperature fluctuation for 30 years measured by a meteorological institute near the bridge. It can be seen that yearly temperature growth is 5 percent and a standard deviation of the yearly temperature fluctuation is approximately 5 percent.

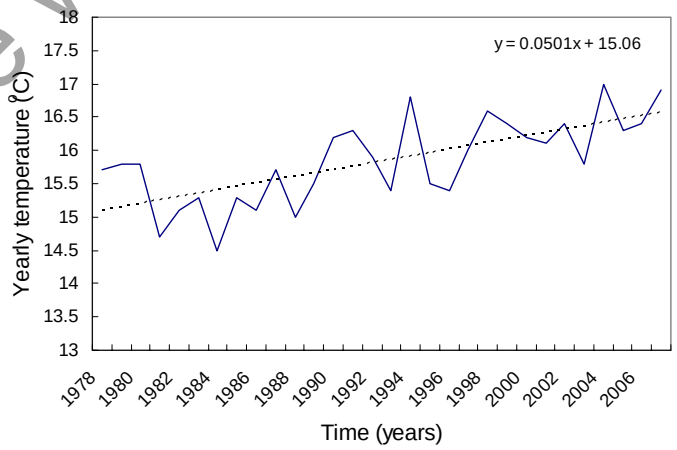

Figure 3 Yearly temperature fluctuation near the bridge.

The average yearly traffic volume growth assumes that the traffic growth rate is 3 percent and a standard deviation of the traffic growth rate is 2 percent.

Step 3: Calculate hourly temperatures, elastic moduli of asphalt, and stress reduction. In order to calculate stress reduction factors, the average hourly air temperature with a time stamp, compiled from the nearest observatory of the meteorological institute, is used to form the cumulative hourly temperature functions, as shown in Figure 4. The horizontal axis represents cumulative hours from 1am, 1 January to 12am 31 December. The maximum, minimum, and average values of the temperatures are 37.9 ^{o}C, -3.7 ^{o}C, and 16.5 ^{o}C respectively. Figure 5 shows representative examples in three-day hourly temperature variation in summer and winter. The one-day temperature variation of 11.8 ^{o}C (37.9-26.1) in summer is almost the same as that of 11.5 ^{o}C (7.8 -(-3.7)) in winter. It can be seen there are distinct temperature variations seasonally and also daily. The hourly temperature values for the calculations are obtained by fitting the field-measured temperature distribution above using Monte Carlo Simulation (MCS), as shown in Figure 6.

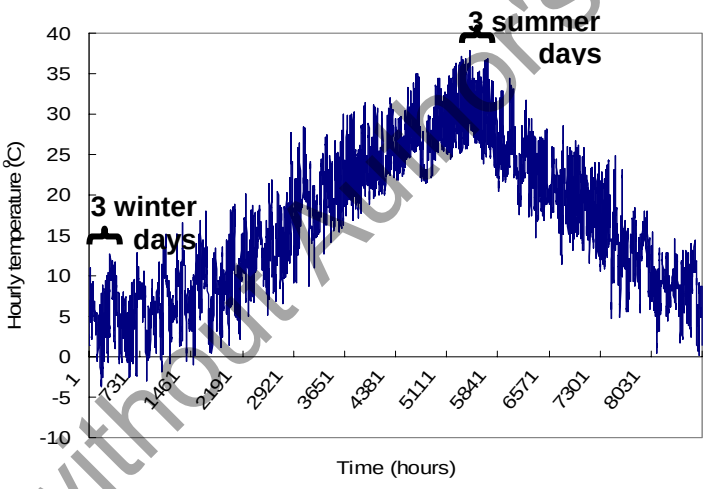

Figure 4 Hourly temperature measured for one year in 2006.

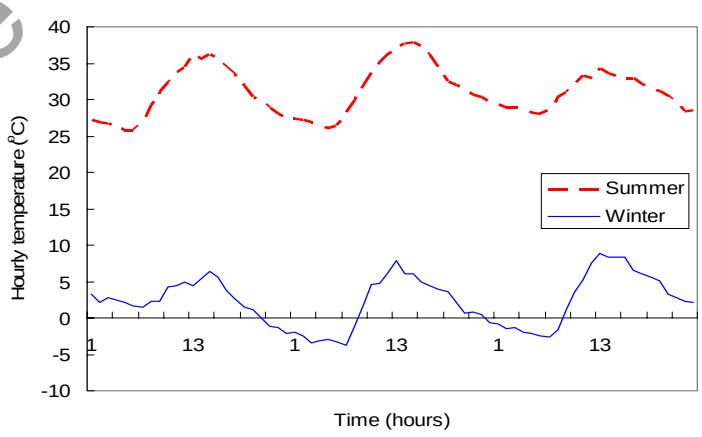

Figure 5 Hourly temperature for three summer, and for three winter days.

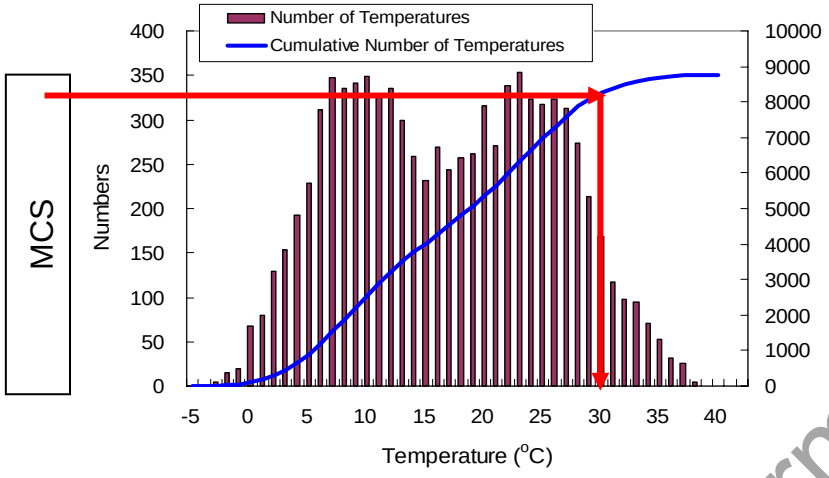

Figure 6 Fitting field-measured temperature distribution using the MCS.

The stress reductions due to the surfacings on orthotropic steel decks are applied to the lifetime calculation. Surfacing materials are generally viscoelastic to plastic, and behave elastically at lower temperatures. The stiffness of most surfacings strongly depends on temperature. Shear slip sometimes occur at the interface between the deck plate and the surfacings with a soft bonding layer. However, surfacing can contribute to the deck rigidity and reduce stress concentration due to local bending of the steel deck plate.

It is assumed for the calculations that there is no difference between asphalt temperature and air temperature. Equation 3 for the asphalt stiffness as a function of the temperature is used to obtain elastic moduli of stone mastic asphalts (SMA), E_{SMA}, (Jong 2006)

$$E_{SMA} = 16956 - 589T \quad \text{(MPa)} \tag{3}$$

where T = the temperature of asphalt (°C).The stress reduction factors are defined as the ratio of the stiffness in the steel deck plate with asphalt surfacing and the stiffness in the steel deck plate without asphalt surfacing, as shown in Equation 4. No composite action between the steel deck plate and the asphalt surfacing is considered (Jong 2006)

$$Sr = \frac{E_{steel} I_{steel}}{E_{steel} I_{steel} + E_{SMA} I_{SMA}} \tag{4}$$

where E_{steel} = the elastic moduli of the steel (210,000 MPa); I_{steel} = the moment of inertia of the steel (e.g. $bh^3/12=b\text{x}12^3/12=144b$ mm^4); I_{SMA} = the moment of inertia of the SMA (e.g. $bh^3/12=b\text{x}80^3/12=42{,}667b$ mm^4).

Step 4: Calculate axle weights, and transverse positions of axle loads. Two sets of traffic data are used to calculate the one-year axle weights on the bridge. The traffic count near the bridge showed that the total daily traffic in 2005 was 75,000 in two lanes, with 20 percent being trucks. Additionally, the one-day amount of 2975 trucks and 8406 axle weights of trucks with time stamps were compiled from the nearest toll gate using axle load scales. This data is used to form the cumulative number of

cycles of axle weights. The daily cycles of 8,406 axle weights are divided into 5 kN sections to indicate the number of cycles in a weight range, as shown in Figure 7. The maximum, minimum, and average values of the axle weights were 217 kN, 9 kN, and 50 kN respectively. Figure 8 shows a time distribution of axle loading using the same one-day axle weight data. Not surprisingly, there is a lot of traffic in the daytime, from 7:00 to 17:00 hours. The morning and evening rush periods can also be seen.

The one-year axle weight data at the bridge is found using Monte Carlo simulation, to fit the field measured axle weight distribution at the toll gate, and to multiply the number of axle weights at the toll gate by 1.8. To adjust axle weight distribution at the toll gate to that at the bridge, this value is obtained from 75000 / 2 lanes x 20 percent trucks x 70 percent in outer lane / 2975 trucks = 1.8 assuming that 70 percent trucks go through in the outer lane.

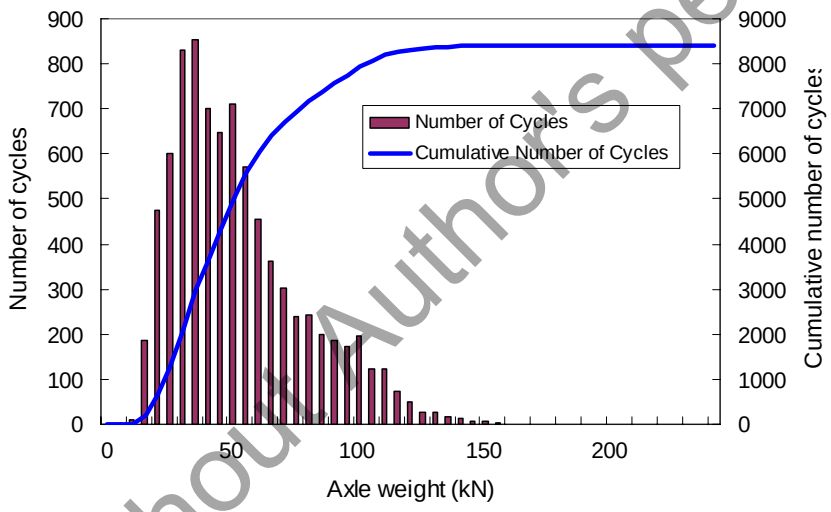

Figure 7 Field measured one-day axle weight distribution.

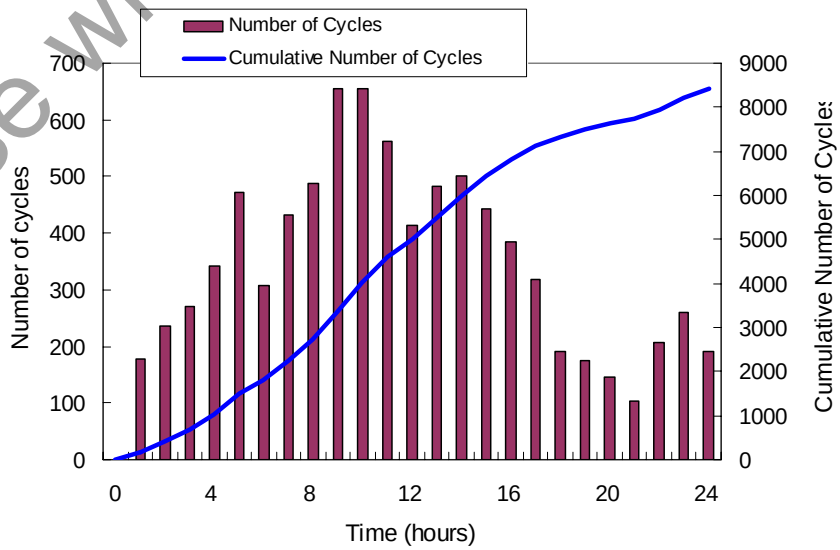

Figure 8 Field measured one-day time distribution of axle loading.

The axle loads of vehicles are spread in the transverse direction over the orthotropic steel bridge deck. Eurocode (EN1991-2 2003) models this transverse distribution in 5 blocks each 100 mm wide with 7 , 18 , 50 , 18 , and 7 percent, as shown in Figure 9. In this assessment, a centre line of this frequency transverse distribution is assumed to move randomly from the deck plate at the crossbeam location (point A in the figure) to the midpoint deck plate between the crossbeam locations (point A and B), because a stress range at point A will be calculated for the assessment.

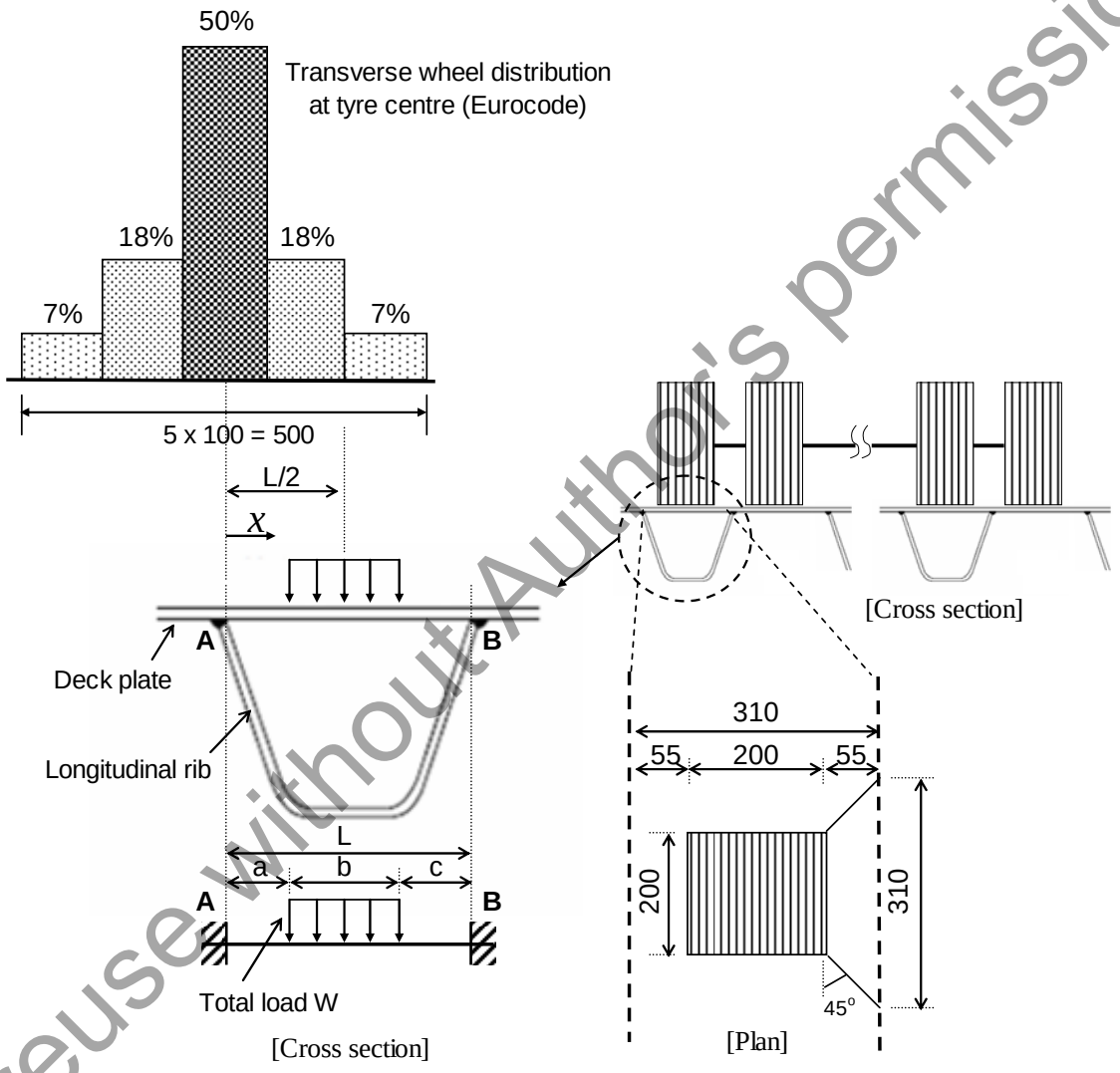

Figure 9 Axle loading positions and models for stress range calculations.

Step 5: Calculate stress ranges from the axle weight data. For the stress range calculation at the crack location A, Figure 9 illustrates the mechanical model. The deck plate between the two webs of the longitudinal rib is modelled as a simple fixed end beam. The span of the beam is the distance between the roots of the two longitudinal rib-to-deck welds. For the deck plate crack at the intersection of the crossbeam, the deck plate, and the longitudinal rib web, a fixed end beam is

considered to be a appropriate model because the crossbeam, the deck plate, and the longitudinal rib web are welded together at the intersection (Jong 2006). With selected type of tyre and rib-to-deck-weld span, the moment at the location A, M_A (Nmm), is given by

$$M_A = \frac{(AW \times 1000)}{12L^2 b}\left[(b+c)^3(4L-3b-3c) - c^3(4L-3c)\right] \quad (5)$$

where AW = quarter of axle weight (kN); a = 0 (when $x < w/2$), $x - w/2$ (when $w/2 < x$); $b = x + w/2$ for (when $x < w/2$), w (when $w/2 < x < L - w/2$), $L - x + w/2$ (when $L - w/2 < x$); $c = L - x - w/2$ (when $x < L - w/2$), 0 (when $L - w/2 < x$); x = randomly selected tyre centre between point A and midpoint AB as Eurocode distribution at selected tyre centre (mm); L = span of a deck plate between rib-to-deck welds (mm) (e.g. 310 mm); w = tyre width (mm) (assuming 200 mm in BS5400:1980). Based on the previous calculations, the stress range at the location A, σ (MPa), is given by

$$\sigma = \frac{M_A}{I} \times y \times Sr \quad (6)$$

where y = perpendicular distance from the neutral axis (mm)(e.g. $y/2 = 12/2 = 6$ mm); I = moment of inertia about the neutral axis (mm^4)(e.g. $bh^3/12=310x12^3/12=4.46x10^4$ mm^4) assuming a 200 mm width wheel load is located in the centre transversely and a load distribution angle of 45^o to the horizontal as shown above, the load distribution in a longitudinal rib-to-deck weld is 310 mm long.

Step 6: Calculate damage from the stress range data. For the damage calculation from the stress range varied in a random manner, the Palmgren-Miner linear cumulative damage rule, commonly called Miner's rule, is used. The number of cycles, N, of any one stress range S, obtained from step 1, are then added up to calculate hourly damage D_h.

$$D_h = \sum \frac{1}{N_i} = \frac{1}{N_1} + \frac{1}{N_2} + \frac{1}{N_3} + \cdots\cdots + \frac{1}{N_n} \quad (7)$$

where N_1, N_2, N_3,…N_n = number of cycles to failure of a stress range obtained from Step 1 in each hour. This hourly damage, D_h, is then added up to calculate yearly damage D_y.

$$D_y = \sum_{i=1}^{24} \sum_{j=1}^{365} D_{h(i,j)} \quad (8)$$

Step 7: Calculate fatigue lifetime from the damage data. The one-year-damage, D_y, obtained in Step 6 is used to calculate a fatigue lifetime until the sum of all these values is 1 considering the traffic growth rate in Step 2.

$$\sum_{i=1}^{t} D_y \times 1.8 \times (1+TGR)^i = 1 \quad (9)$$

where t = fatigue lifetime (years); TGR = traffic growth rate (in Step 2); 1.8 = constant (in Step 4).

Step 8: Repeat Steps 1 to 7 for a fatigue lifetime distribution. Calculations from step 1 to step 7 are repeated to yield a distribution of the fatigue lifetime. Figure 10 shows an example result of the calculation with one thousand samples to predict the fatigue lifetime for the surfaced deck plate under Detail Category 125. The calculation results are divided into 3 month sections to illustrate probability of failure of cracking in a time range described in terms of a probability density function (PDF) and a cumulative density function (CDF). The mean of fatigue lifetime is 46.1 years. The maximum, minimum, and standard deviation of fatigue lifetime are 185.0, 10.3, and 24.3 years respectively. It can be seen that probability of failure of cracking in 10 years is very close to 0 percent.

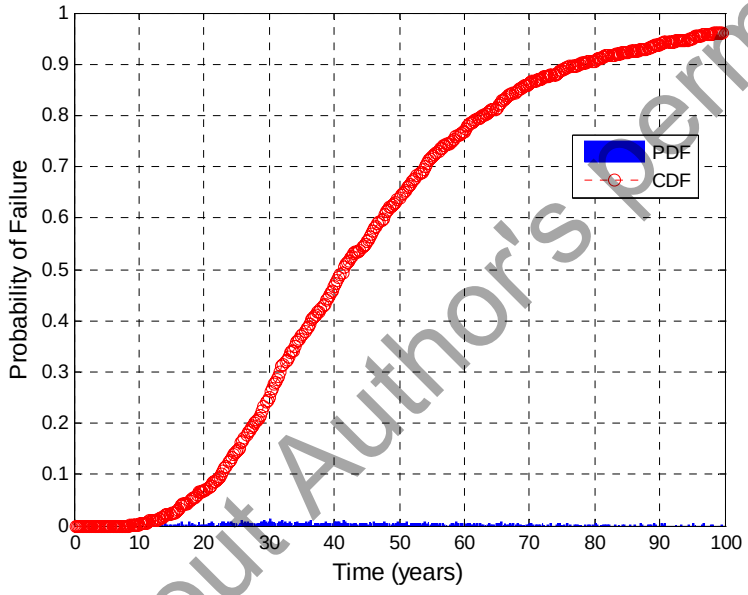

Figure 10 Probability of failure of cracking for the deck plate with 80 mm asphalt under Detail Category 125 (1,000 simulations).

Results and Discussion

Three example results are obtained using a mostly probabilistic methodology. Three Detail Categories of 125, 100, and 71 discussed in the previous section are applied. Figure 11 shows an example result of the calculation with one thousand samples to predict the fatigue lifetime for the surfaced deck plate under Detail Category 100 described as critical regions at the longitudinal rib-to-deck welded joint in prEN 1993-2 (2005). The mean fatigue lifetime is 23.8 years. The maximum, minimum, and standard deviation of fatigue lifetime are 88.9, 3.9, and 12.3 years respectively. It can be seen that probability of failure of cracking in 10 years is approximately 8 percent. Figure 12 shows an example result of the calculation with one thousand samples for the surfaced deck plate under Detail Category 71 described for orthotropic decks with closed longitudinal stiffeners given in EN 1993-1-9 (2005). The mean fatigue lifetime is 11.1 years. The maximum, minimum, and standard deviation of fatigue lifetime are 71.1, 1.6, and 8.6 years respectively. It can be seen

that probability of failure of cracking in 10 years is very close to 60 percent. The median fatigue lifetime for the Detail Categories of 125, 100, and 71 are 40.6, 21.3, and 8.7 years respectively.

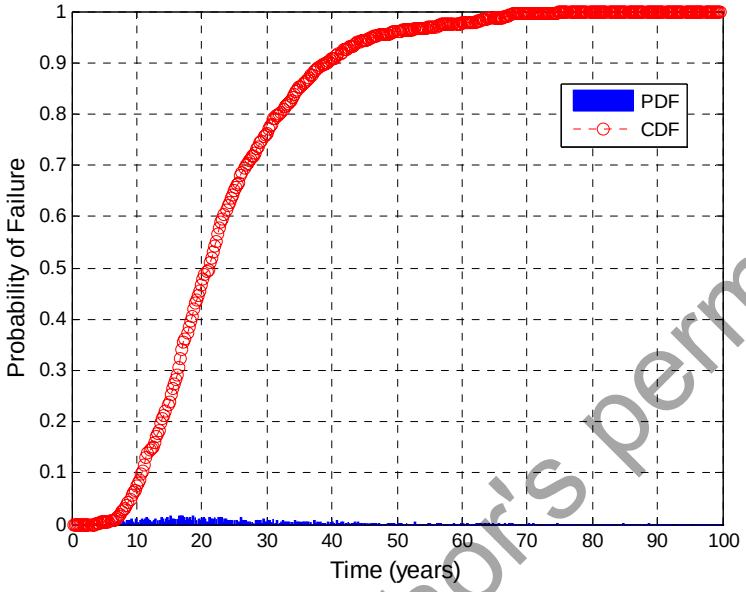

Figure 11 Probability of failure of cracking for the deck plate with 80 mm asphalt under Detail Category 100 (1,000 simulations).

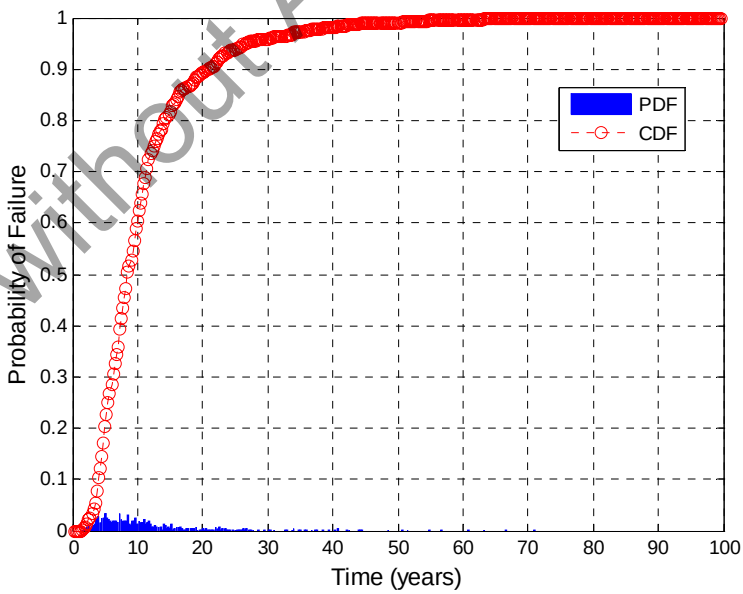

Figure 12 Probability of failure of cracking for the deck plate with 80 mm asphalt under Detail Category 71 (1,000 simulations).

It should be noted that cracking was found to occur at the rib-to-deck welded joint of the Shinhamadera Bridge almost 10 years after it was opened. The category

associated with this detail is more likely to be the Detail Category 71 than the other categories. However it should be noted that the cracking strongly depends on fabrications and welding processes. Therefore the Detail Category 125 could be considered reasonable and proper for rib-to-deck welded connection of the orthotropic steel bridge deck, which has been recommended by Kolstein (2007). This particular detail was considered to have been deficient as similar cracking elsewhere in the bridge did not occur at the same time. Based on the curve under Detail Category 125, there is a significant probability (50 percent) that cracking will occur in the next 30 years.

Figure 13 shows an example result of the calculation with one thousand samples to predict the fatigue lifetime for the unsurfaced deck plate under Detail Category 125. The mean fatigue lifetime is 6.5 years. The maximum, minimum, and standard deviation of fatigue lifetime are 30.7, 1.2, and 3.4 years respectively. It can be seen that probability of failure of cracking in 10 years is approximately 87 percent. Under the Detail Category 125, the median fatigue lifetime for the unsurfaced deck plate is 5.9 years, which is much smaller than 40.6 years for the deck plate with 80 mm asphalt. It can be clearly seen that there is a significant surfacing effect for fatigue lifetime due to stress reductions in the deck plates.

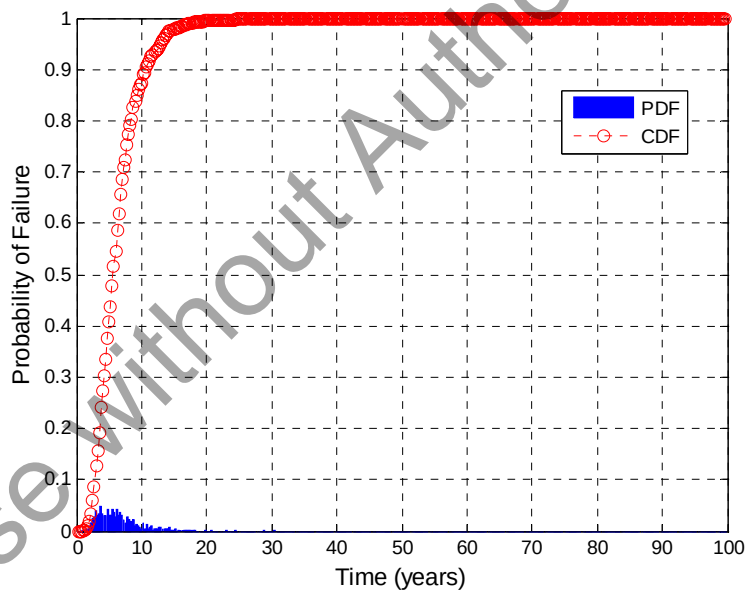

Figure 13 Probability of failure of cracking for the deck plate without surfacing under Detail Category 125 (1,000 simulations).

For future works, better models and qualifications of the fatigue category are required to more accurately evaluate the lifetime to failure of cracking. Surfacing characteristics at different asphalt temperatures are also being characterised. Further development of this assessment procedure will allow for bridge life cycle cost analysis and will include the effects of surfacing performance, deterioration, and replacement.

Conclusions

1. A simple but rigorous probabilistic methodology for fatigue lifetime has been developed. The probabilistic fatigue lifetime estimation model has been developed taking into account conventional fatigue lifetime estimation methods based on the Miner's Rule with *S-N* curves. The methodology allows for the introduction of the asphalt surfacing effect considering seasonal and daily temperature variations as the stress reduction at the rib-to-deck welded joints with the crossbeam in the orthotropic steel bridge decks.
2. The method has estimated fatigue lifetime within ranges broadly consistent with a real bridge lifetime, but is being updated to provide more realistic results as to become a decision support tool for life cycle cost analysis.

Acknowledgement

The authors wish to thank the Hanshin Expressway Co. Ltd and the New Zealand Heavy Engineering Research Association (HERA) for providing support for this work.

References

Beamish, M., Tindall, P., and Billings, I. "Auckland Harbour Bridge Fatigue Assessments." *Austroads 6th Bridge Conference 2006*, Perth.

BSI. (1980). *Steel, concrete and composite bridges, code of practice for fatigue (BS 5400: Part 10).* British Standards Institution (BSI), London.

Cornell, C. A., and Krawinkler, H. (2000). "Progress and Challenges in Seismic Performance Assessment." *Peer Center News*, 3(2).

EN1991-2. (2003). *Eurocode 1: Actions on structures – Part 2: Traffic loads on bridges*, Brussels, Belgium.

EN1993-1-9. (2005). *Eurocode 3: Design of steel structures – Part 1-9: Fatigue*, Brussels, Belgium.

Jong, F. B. P., de (2006). "Renovation techniques for fatigue cracked orthotropic steel bridge decks," Delft University of Technology, Delft

Kolstein, M. H. (2007). "Fatigue Classification of Welded Joints in Orthotropic Steel Bridge Decks," Delft University of Technology, Delft

Miki, C. (2006). "Fatigue Damage in Orthotropic Steel Bridge Decks and Retrofit Works." *International Journal of Steel Structures*, 6, 255-267.

prEN1993-2. (2005). *Eurocode 3: Design of steel structures – Part 2: Steel Bridges*, Brussels, Belgium.

Sugioka, K., Tabata, A., Takada, Y., and Yamamura, K. "Investigation and reinforcement for fatigue crack damages on an orthotropic steel deck bridge." *Pacific Structural Steel Conference 2007*, Wairakei, New Zealand.

Wolchuk, R. (1990). "Lessons from Weld Cracks in Orthotropic Decks on Three European Bridges." *Journal of Structural Engineering*, 116(1), 75-84.